The Canadian Mineralogist
Vol. 46, pp. 183-193 (2008)
DOI: 10.3749/canmin.46.1.183

GAUDEFROYITE, $Ca_8Mn^{3+}_6[(BO_3)_6(CO_3)_2O_6]$: HIGH-TEMPERATURE CRYSTAL STRUCTURE

SYTLE M. ANTAO[§]

Advanced Photon Source, Argonne National Laboratory, Argonne, Illinois 60439, USA

ISHMAEL HASSAN

Department of Chemistry, University of the West Indies, Mona, Kingston 7, Jamaica

ABSTRACT

The structural behavior of gaudefroyite, $Ca_8Mn^{3+}_6[(BO_3)_6(CO_3)_2O_6]$, was determined by using Rietveld refinements based on synchrotron powder X-ray-diffraction data from 25 to 486°C. The structure was also refined at 25°C using synchrotron high-resolution powder X-ray-diffraction (HRPXRD) data that gave the pseudohexagonal unit-cell parameters *a* 10.60791(2), *c* 5.88603(1) Å, and *V* 573.605(2) Å^3 at room temperature. The expansion of the gaudefroyite structure is nearly isotropic and is caused mainly by an increase in the Ca1–O3 distance. The volume change from 25° to 486°C is 2.2(2)%. Beyond 486°C, significant changes were observed in the X-ray-diffraction traces; they indicate the formation of a minor second phase that exsolved from the host gaudefroyite.

Keywords: gaudefroyite, high-temperature structure, exsolution, Rietveld refinements, synchrotron radiation.

SOMMAIRE

Nous avons déterminé le comportement structural de la gaudefroyite, $Ca_8Mn^{3+}_6[(BO_3)_6(CO_3)_2O_6]$, au moyen d'affinements Rietveld de données en diffraction X sur poudre obtenues entre 25 et 486°C avec rayonnement synchrotron. La structure a aussi été affinée à 25°C en utilisant des données de haute résolution obtenues avec rayonnement synchrotron; les paramètres réticulaires de la maille pseudo-hexagonale sont *a* 10.60791(2), *c* 5.88603(1) Å, et *V* 573.605(2) Å^3 à température ambiante. L'expansion de la structure est presque isotrope, et résulte surtout de l'augmentation de la distance Ca1–O3. Le changement du volume en allant de 25° à 486°C est 2.2(2)%. Au delà de 486°C, nous observons des changements importants dans le spectre de diffraction X; ils indiquent la formation d'une faible quantité d'une seconde phase, exsolvée de la gaudefroyite hôte.

(Traduit par la Rédaction)

Mots-clés: gaudefroyite, structure à température élevée, exsolution, affinements de Rietveld, rayonnement synchrotron.

INTRODUCTION

Gaudefroyite, $Ca_8Mn^{3+}_6[(BO_3)_6(CO_3)_2O_6]$, Z = 1, occurs in the hydrothermal manganese deposits, Tachgagalt, Anti-Atlas Mountains, Morocco (Jouravsky & Permingeat 1964), and in the Kalahari manganese field, South Africa (Beukes *et al*. 1993, Hochleitner 1986). In South Africa, gaudefroyite occurs either as vein fillings, where it is associated with barite, calcite, manganite, and hydrogrossular, or as massive ores, where it is associated with manganite, bixbyite, braunite, hausmannite and hematite. These mineral associations indicate a high temperature and a low pressure of formation; gaudefroyite and barite were formed during an episode of boron metasomatism (Beukes *et al*. 1993).

At ambient pressure, there is no information available on the high-temperature structure of gaudefroyite. Streaked satellite reflections occur in gaudefroyite. The purpose of this study is to examine the structural evolution of gaudefroyite with temperature for possible transitions that may occur on heating, or on the loss of the streaked satellite reflections. We find that the structure refines well from 25 to 486°C; thereafter, a minor second phase exsolves from the host phase.

§ *E-mail address*: sytle.antao@anl.gov

Background Information

The structure of gaudefroyite was determined and refined by Granger & Protas (1965), Yakubovich *et al*. (1975), and Hoffmann *et al*. (1997). Hoffmann *et al*. (1997) presented their preferred structural model in space group $P6_3/m$. The structure of gaudefroyite contains infinite columns formed by *trans-trans*-connected edge-sharing $Mn^{3+}O_6$ octahedra that are cross-linked by triangular BO_3^{3-} groups to form two different types of channels (Figs. 1a, b). The CO_3^{2-} groups that are located in the center of the wide channels locally violate the mirror plane perpendicular to the ***c*** axis, such that the CO_3^{2-} groups may be disordered (Hoffmann *et al*. 1997).

Gaudefroyite is both structurally and compositionally similar to cancrinite with regards to the CO_3^{2-} group and its surroundings (Hassan 2000). In cancrinite, the CO_3^{2-} groups are ordered within identical channels and produce a superstructure (Grundy & Hassan 1982, Hassan 1996, Hassan & Buseck 1992). Gaudefroyite shows strong, continuous streaked reflections in selected-area electron-diffraction (SAED) patterns, an indication that the symmetry of gaudefroyite is lower than hexagonal (Hassan 2000). The CO_3^{2-} groups in the large 6_3 channels are ordered in two different ways, and this pattern of order gives rise to two different types of channels, A and B. The A and B channels occur in a 1:1 ratio, and these channels are partially ordered and give rise to the continuous streaked reflections in SAED patterns (Hassan 2000). A DTA–TG study of gaudefroyite shows that the loss of CO_2(g) in gaudefroyite occurs at 1053°C (Hassan & Duane 1999).

Experimental Methods

The sample used in this study is from the Wessels mine, Kalahari manganese field, South Africa. Pure and well-developed crystals of gaudefroyite occur in association with barite, calcite, manganite, and hydrogrossular. Crystals of gaudefroyite were hand-picked under a binocular microscope and finely ground using an agate mortar and pestle for the X-ray diffraction experiments.

High-resolution powder X-ray diffraction (*HRPXRD*)

The structure at 25°C was refined using HRPXRD data from beam-line 11-BM, Advanced Photon Source, Argonne National Laboratory. The sample was loaded into a kapton capillary and rotated during the experiment at a rate of 90 rotations per second. The data were collected to a maximum 2θ of about 45° with a step size of 0.001° and a step time of 0.3 s/step. Beamline optics consists of a platinum-coated collimating mirror, a dual Si (111) monochromator, and a platinum-coated vertically focusing mirror. The HRPXRD traces were

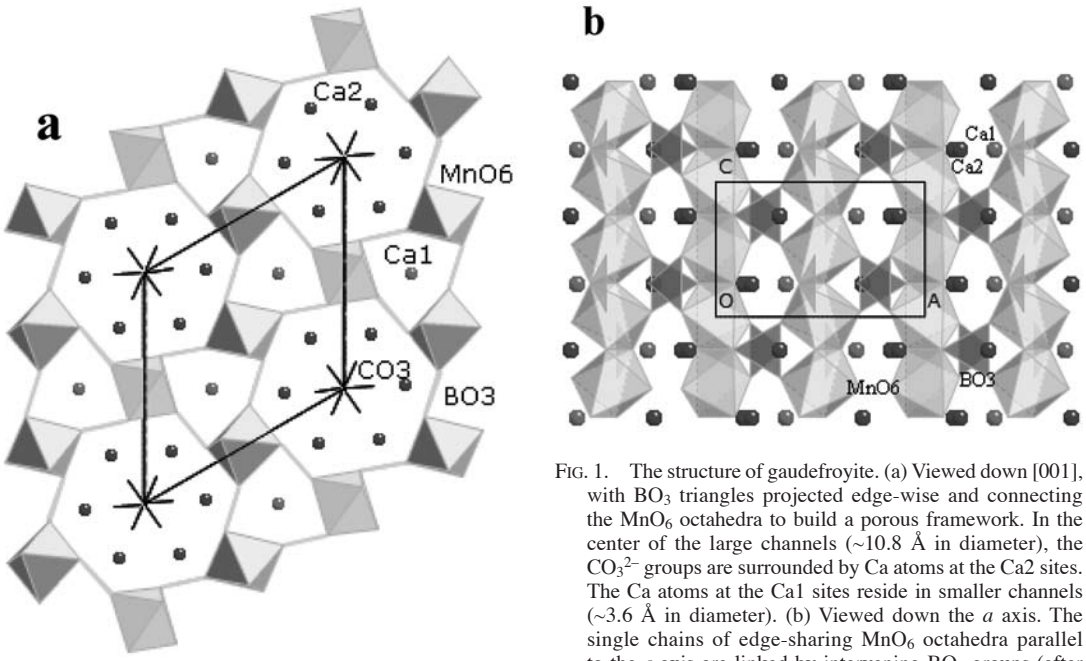

FIG. 1. The structure of gaudefroyite. (a) Viewed down [001], with BO_3 triangles projected edge-wise and connecting the MnO_6 octahedra to build a porous framework. In the center of the large channels (~10.8 Å in diameter), the CO_3^{2-} groups are surrounded by Ca atoms at the Ca2 sites. The Ca atoms at the Ca1 sites reside in smaller channels (~3.6 Å in diameter). (b) Viewed down the *a* axis. The single chains of edge-sharing MnO_6 octahedra parallel to the *c* axis are linked by intervening BO_3 groups (after Hoffmann *et al*. 1997).

collected with twelve silicon-crystal analyzers, which increase detector efficiency and reduce the angular range to be scanned, and therefore, allows rapid acquisition of data. A silicon and alumina NIST standard (ratio of $^1/_3Si:^2/_3Al_2O_3$) was used to calibrate the detector response, zero offset, and to determine the wavelength used in the experiment [$\lambda = 0.40167(2)$ Å]. Data were merged by interpolating measured counts onto a regularly spaced grid and by applying corrections for small differences in wavelength (~1 eV).

High-temperature synchrotron powderX-ray diffraction

High-temperature synchrotron X-ray powder-diffraction experiments were performed at beam-line X7B of the National Synchrotron Light Source at Brookhaven National Laboratory. The powdered sample was loaded into a quartz capillary (diameter = 0.5 mm, open to air at one end) and was oscillated during the experiment over a θ range of 10°. The high-T X-ray data were collected using *in situ* synchrotron radiation [$\lambda = 0.9212(4)$ Å] at ambient pressure and from 25 to 845°C. Elevated T was obtained using a horseshoe-shaped heater and a thermocouple element near the capillary. The temperature was calibrated using the 811 and 982°C phase-transition temperatures of synthetic $BaCO_3$ (Hodgman 1955). Data were collected at a heating rate of about 7°C/min. The data were collected over regular intervals of about 17°C to a maximum 2θ of about 50° [$(\sin\theta/\lambda) < 0.46$ Å^{-1}]. An image plate (IP) detector (Mar345, 2300 × 2300 pixels) mounted perpendicular to the beam path was used to collect full-circle Debye–Scherrer rings with an exposure time of 10 s. An external LaB_6 standard was used to determine the sample-to-detector distance, wavelength, and tilt of the IP. The diffraction patterns recorded on the IP were integrated using the FIT2D program to produce conventional *I*–2θ traces (Hammersley *et al*. 1996).

Rietveld Refinements of the Structure

Several X-ray traces at regular intervals of temperature were modeled using the Rietveld method, as implemented in the GSAS program and using the EXPGUI interface (Larson & Von Dreele 2000, Toby 2001). For the room-temperature structure of gaudefroyite, the starting structural parameters and space group, $P6_3/m$, were taken from Hoffmann *et al*. (1997). The refined coordinates of the atoms were then used as input for the next higher-T structure.

The background was modeled using a Chebyschev polynomial. The reflection-peak profiles were fitted using profile function type-3 in the GSAS program with the refinable coefficients GW, GV, GU, LX and LY. A full-matrix least-squares refinement varying a scale factor, cell parameters, atom coordinates, and isotropic displacement parameters converged rapidly. For the HRPXRD data, all atoms were refined anisotropically, and no constraints were used. For the IP data, isotropic displacement parameters were used, and similar atoms were set to have equal displacement-parameters; for example, the atoms of the CO_3^{2-} groups were constrained to have equal displacement-parameters, and U(C) = U(B). Toward the end of the refinement, all parameters were allowed to vary, and the refinement proceeded to convergence. The number of observed reflections in a typical XRD trace is 186 for the high-T data (1568 for HRPXRD data). Synchrotron X-ray powder-diffraction patterns are shown in Figures 2 to 4, as examples.

Thermal analyses

Simultaneous differential scanning calorimetry (DSC) and thermogravimetry (TG) data were also obtained using a Netzsch STA 449C simultaneous TG and DSC instrument. About 1.56 mg of powdered sample was loaded in an Al_2O_3 crucible. Data were collected in a static air environment, at a heating rate of 10°C/min from 25 to 1200°C. The TG curve was corrected for buoyancy effect, and the DSC curve was corrected for baseline effect. Corrections for buoyancy and baseline effects were obtained in a blank run using empty crucibles that were later used to run the sample in a second run, but the two experimental runs were made under identical conditions. The thermal data were analyzed using the programs provided with the instrument. The DTG and DDSC curves are the derivatives of the TG and DSC curve, respectively.

Results and Discussion

High-temperature XRD traces

In selected-area electron-diffraction (SAED) patterns, fairly strong continuously streaked reflections occur in the gaudefroyite sample used in this study, but such reflections were not observed in the powder XRD traces (Fig. 2; Hassan 2000). However, the XRD traces show significant changes after 486°C, indicating that a structural transition may have occurred (arrows in Fig. 2). The structure could not be refined at temperatures beyond 486°C without excluding the extra reflections that appear in the XRD traces. Moreover, the traces beyond 486°C, and the trace obtained after cooling the sample to room T, could not be indexed in a single crystal-system, particularly the cubic system, as a structure of higher symmetry is expected if a transition occurs. Therefore, the extra reflections in the XRD traces that occur beyond 486°C indicate an exsolved minor second phase within the sample. To rule out the possibility of a polymorphic phase-transition, thermal analyses were carried out using some of the remaining powdered sample.

DSC and TG analyses

A previous DTA and TG study showed that the loss of CO_2(g) in gaudefroyite occurs at 1053°C, and no weight change occurs before 1053°C (Hassan & Duane 1999). The DSC and TG results from this study and the characteristic data are shown in Figure 5. The DSC result shows no phase transition; the loss of CO_2(g) occurs at about 1000°C. However, the TG curve shows a weight increase before the weight loss, which was not observed in the previous study, in which a large sample was used compared to the present study (90.8 mg *versus* 1.56 mg in this study). No obvious phase-transition is observed at about 486°C (Fig. 5), as was indicated by the high-T XRD traces (Fig. 2). The changes observed in the XRD traces beyond 486°C are most likely caused by the appearance of an exsolved minor phase within the host sample. The weight increase in TG could occur from oxidation of Mn^{3+} to form MnO_2 (pyrolusite), Mn_2O_3 (bixbyite), or Mn_3O_4 (hausmannite). We tried to insert the diffraction peaks of these possible phases to see if a match was possible for the non-gaudefroyite diffraction peaks. Pyrolusite and bixbyite can be ruled out, but hausmannite seems like a good candidate for the exsolved phase, as a few diffraction peaks do match.

Unit-cell parameters

From the HRPXRD data at 23°C, the cell parameters (pseudohexagonal cell) obtained in this study are *a* 10.60791(2), *c* 5.88603(1) Å, *V* 573.605(2) Å^3, and they are similar to those reported by others (*e.g.*, Beukes *et al.* 1993, Hoffmann *et al.* 1997). The unit-cell parameters increase linearly with T (Table 1, Fig. 6). The expansion of the *a* and *c* parameters is of similar magnitude, indicating that the expansion is nearly isotropic (Fig. 6d). The volume thermal expansivity for gaudefroyite was obtained by fitting all the cell-volume data simultaneously to the expression:

$$V(T) = V_{Tr} \exp\left[\int_{Tr}^{T} \alpha_V(T)\, dT\right],$$

where V(T) is the volume at any temperature T, V_{Tr} is the volume at reference T, usually room T, and α_V(T) is

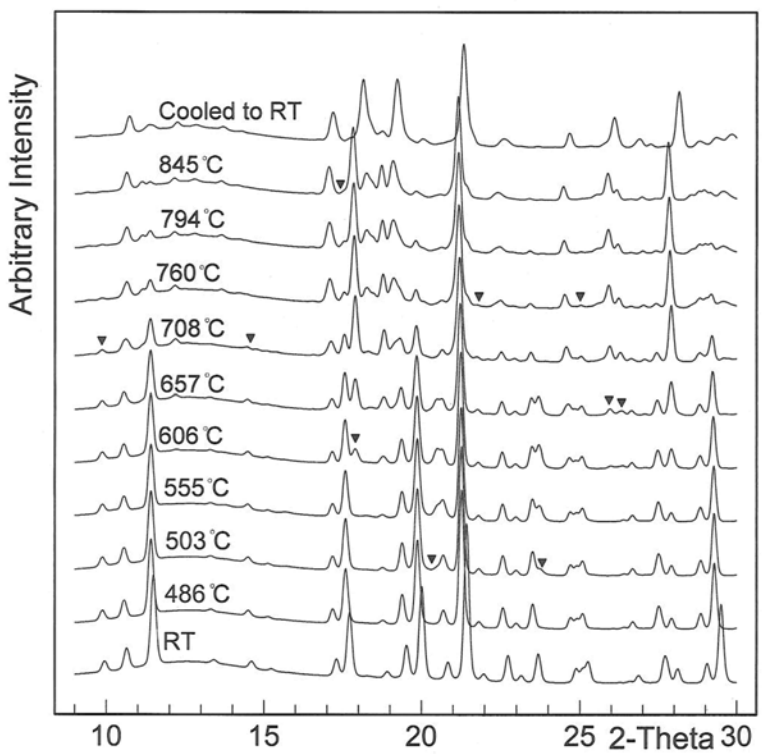

FIG. 2. Stack of XRD traces for gaudefroyite at different temperatures. The arrow heads indicate changes in the traces at temperatures higher than 486°C.

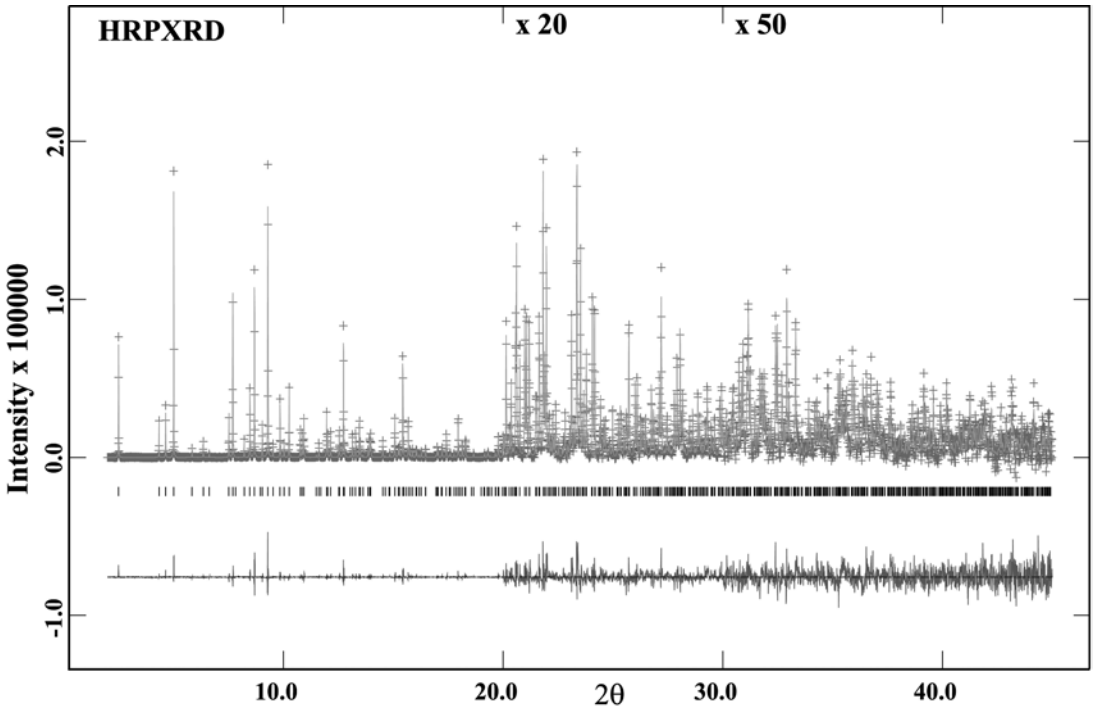

FIG. 3. HRPXRD trace for gaudefroyite, together with the calculated (continuous line) and observed (crosses) profiles. The difference curve ($I_{obs} - I_{calc}$) is shown at the bottom. The short vertical lines indicate the position of allowed reflections. Note that from 20 to 30° 2θ, the intensity is scaled by ×20, and in the interval 30–45° 2θ, it is scaled by ×50 compared to the low-angle region.

TABLE 1. GAUDEFROYITE: UNIT-CELL AND RIETVELD-REFINEMENT DATA

T (°C)	*a* (Å)	*c* (Å)	*V* (Å^3)	$^*R_F^2$
25†	10.60791(3)	5.88603(1)	573.605(2)	0.0562
25	10.60074(9)	5.88402(8)	572.63(1)	0.0233
59	10.60643(9)	5.88761(8)	573.60(1)	0.0248
93	10.61129(9)	5.89062(8)	574.42(1)	0.0222
145	10.61864(9)	5.89528(8)	575.67(1)	0.0243
196	10.62601(9)	5.90008(8)	576.94(1)	0.0211
247	10.63402(9)	5.90520(8)	578.31(1)	0.0242
298	10.64342(9)	5.91056(8)	579.86(1)	0.0243
350	10.65448(9)	5.91703(8)	581.70(1)	0.0250
384	10.65998(9)	5.92041(8)	582.63(1)	0.0238
401	10.66317(9)	5.92221(8)	583.16(1)	0.0238
452	10.67026(9)	5.92616(7)	584.32(1)	0.0237
486	10.67467(9)	5.92984(8)	585.17(1)	0.0287

† Data from HRPXRD. $^*R_F^2$ = R-structure factor based on observed and calculated structure-amplitudes = $[\Sigma F_o^2 - F_c^2)^2 / \Sigma(F_o^2)^2]^{1/2}$.

a function for the volume thermal expansion coefficient: $\alpha_V(T) = a_0 + a_1T + a_2T^{-2}$. Ignoring the quadratic term, for the range 25 to 486ºC, the values: $a_0 = 4.41(\pm 0.17) \times 10^{-5}$/°C and $a_1 = 1.51\ (\pm 0.80) \times 10^{-8}$/°C, were obtained with $V_{Tr} = 572.63(1)$ Å^3 at 25ºC. The volume change from 25 to 486°C amounts to 2.2(2)%.

The structure of gaudefroyite

The general structural features of gaudefroyite have been described in the introduction; the structure at 23°C is similar to that obtained by Hoffmann *et al.* (1997). The structure refines remarkably well to 486°C. The XRD trace obtained at room T after heating is different from that before heating, which indicates that the exsolution that occurred in the sample after 486°C was not reversible.

Some of the isotropic displacement parameters were set equal to each other, for example, those of the O atoms (Table 2). The isotropic displacement parameters have normal values at room T, and they increase smoothly with T (Fig. 7).

The average <Mn–O>, <C–O>, and <B–O> distances are nearly constant with T (Fig. 8a). Therefore, the structural units CO_3, BO_3 and MnO_6 behave as rigid bodies. In the case of the MnO_6 polyhedron, the Mn^{3+} cation displays the (4 + 2) coordination because of the Jahn–Teller effect. The two Mn–O2 bonds are much longer than the other four (Mn–O1 and Mn–O3) bonds; the latter sets are nearly equal to each other (Table 3,

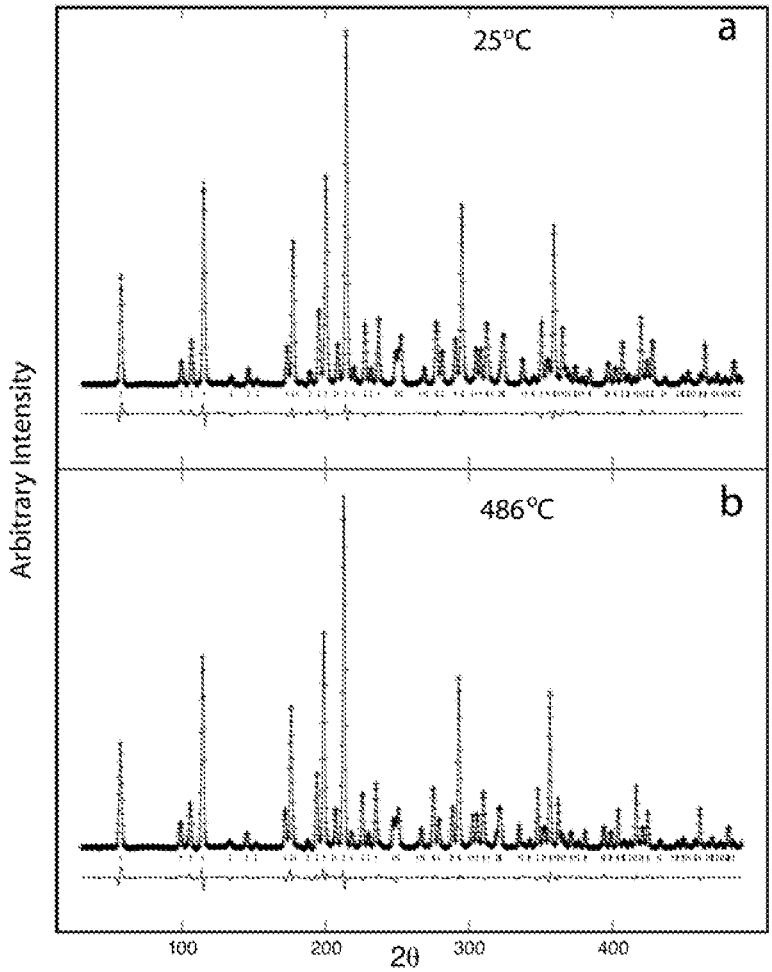

FIG. 4. Comparison of the XRD traces for gaudefroyite at (a) 25 and (b) 486°C, together with the calculated (continuous line) and observed (crosses) profiles. The difference curve ($I_{obs} - I_{calc}$) is shown at the bottom. The short vertical lines indicate the position of allowed reflections.

TABLE 2a. GAUDEFROYITE: COORDINATES AND DISPLACEMENT PARAMETERS OF ATOMS (× 100 Å^2), FROM HRPXRD

Atom	sof	*x*	*y*	*z*	U_{eq}	U_{11}	U_{22}	U_{33}	U_{12}	U_{13}	U_{23}
Ca1	1	1/3	2/3	0.25	0.94	1.14(6)	1.14(6)	0.51(7)	0.57(3)	0	0
Ca2	1	0.1332(1)	0.8323(1)	0.25	0.81	1.32(7)	1.08(7)	0.53(4)	0.93(6)	0	0
B	1	0.2180(8)	0.7629(7)	0.75	0.47	1.4(4)	0.32(30)	0.26(20)	0.64(24)	0	0
Mn	1	0	0.5	0	0.60	0.53(3)	0.46(4)	0.54(3)	0.02(4)	-0.24(3)	0.28(3)
C	0.5	0	0	0.0772(23)	3.92	4.6(5)	4.6(5)	2.5(8)	2.29(27)	0	0
O1	1	0.0932(3)	0.4735(3)	0.25	0.94	2.12(22)	0.36(20)	0.17(17)	0.04(17)	0	0
O2	1	0.3211(4)	0.9191(4)	0.75	1.38	2.01(21)	2.30(22)	1.57(18)	2.54(20)	0	0
O3	1	0.3037(2)	0.4704(3)	0.5399(3)	1.71	1.04(14)	3.09(20)	0.55(14)	1.23(14)	-0.15(10)	-0.09(10)
O_c	0.5	0.0531(5)	0.9044(5)	0.5745(8)	5.57	0.17(30)	4.84(43)	4.66(41)	-2.96(28)	-1.30(24)	3.85(34)

TABLE 2b. GAUDEFROYITE: POSITIONS AND ISOTROPIC DISPLACEMENT PARAMETERS[§] (× 100 Å^2) OF ATOMS

Atoms/T°C		25	59	93	145	196	247	298	350	384	401	452	486
Ca1	*U*	1.05(5)	1.19(5)	1.33(5)	1.48(5)	1.58(5)	1.83(5)	1.99(5)	2.21(6)	2.24(6)	2.31(6)	2.49(6)	2.63(6)
Ca2	*x*	0.1319(2)	0.1320(2)	0.1323(2)	0.1323(2)	0.1325(2)	0.1330(2)	0.1332(2)	0.13372(20)	0.1339(2)	0.1341(2)	0.1343(2)	0.1345(2)
	y	0.8316(2)	0.8317(2)	0.8319(2)	0.8319(2)	0.8322(2)	0.8323(2)	0.8323(2)	0.83245(21)	0.8326(2)	0.8326(2)	0.8328(2)	0.8328(2)
B	*x*	0.2170(13)	0.2166(12)	0.2169(13)	0.2164(12)	0.2178(13)	0.2161(12)	0.2167(13)	0.2170(13)	0.2175(14)	0.2171(13)	0.2179(13)	0.2190(16)
	y	0.7725(14)	0.7717(13)	0.7728(14)	0.7720(13)	0.7740(14)	0.7728(14)	0.7741(14)	0.7746(15)	0.7751(15)	0.7750(15)	0.7758(15)	0.7789(17)
	U	0.24(24)	0.36(24)	0.37(24)	0.43(24)	0.57(24)	0.68(24)	0.97(24)	1.13(25)	1.02(25)	1.01(25)	1.27(25)	1.83(28)
Mn	*U*	0.20(4)	0.30(4)	0.37(4)	0.46(4)	0.49(4)	0.64(4)	0.73(4)	0.86(4)	0.88(4)	0.92(4)	1.03(4)	1.17(5)
C	*z*	0.0630(26)	0.0601(27)	0.0610(27)	0.0587(27)	0.0565(28)	0.0581(28)	0.0549(30)	0.0522(31)	0.0518(32)	0.0518(31)	0.0493(32)	0.050(4)
O1	*x*	0.0919(4)	0.0923(4)	0.0921(4)	0.0926(4)	0.0926(4)	0.0927(4)	0.0928(4)	0.09273(43)	0.0928(4)	0.0925(4)	0.0925(4)	0.0919(5)
	y	0.4734(4)	0.4738(4)	0.4738(4)	0.4743(4)	0.4744(4)	0.4747(4)	0.4753(4)	0.4756(4)	0.4759(4)	0.4758(4)	0.4759(4)	0.4752(4)
	U	2.31(7)	2.39(7)	2.55(7)	2.70(7)	2.88(7)	3.04(7)	3.18(7)	3.42(8)	3.51(8)	3.62(8)	3.78(8)	3.97(9)
O2	*x*	0.3198(5)	0.3200(5)	0.3198(5)	0.3199(5)	0.3198(5)	0.31890(46)	0.3188(5)	0.31846(48)	0.3186(5)	0.3185(5)	0.3183(5)	0.3191(5)
	y	0.9194(5)	0.9195(5)	0.9196(5)	0.9196(5)	0.9196(6)	0.9191(6)	0.9193(6)	0.9195(6)	0.9196(6)	0.9195(6)	0.9193(6)	0.9189(6)
O3	*x*	0.3085(3)	0.3082(3)	0.3083(3)	0.3081(3)	0.3083(3)	0.3079(3)	0.3078(3)	0.30799(33)	0.3079(3)	0.3079(3)	0.3075(3)	0.3068(4)
	y	0.4758(3)	0.4755(3)	0.4755(3)	0.4753(3)	0.4753(3)	0.4749(4)	0.4747(4)	0.4747(4)	0.4746(4)	0.4744(4)	0.4738(4)	0.4731(4)
	z	0.5395(5)	0.5398(5)	0.5401(5)	0.5400(5)	0.5406(5)	0.5409(5)	0.5413(5)	0.5417(5)	0.5419(5)	0.5419(5)	0.5423(5)	0.5422(6)
O_C	*x*	0.0587(12)	0.0590(12)	0.0589(12)	0.0591(12)	0.0593(13)	0.0591(13)	0.0591(13)	0.05851(135)	0.0586(14)	0.0582(14)		0.0608(17)
	y	0.9152(11)	0.9155(11)	0.9153(11)	0.9156(11)	0.9152(11)	0.9160(11)	0.9159(12)	0.9157(12)	0.9152(12)	0.9154(12)	0.9153(12)	0.9165(15)
	z	0.5705(9)	0.5706(9)	0.5697(9)	0.5692(9)	0.5680(9)	0.5669(10)	0.5661(10)	0.5642(10)	0.5620(10)	0.5608(10)	0.5583(10)	0.5534(11)

[§] Constraints: $U_{Ca1} = U_{Ca2}$; $U_{O1} = U_{O2} = U_{O3} = U_{OC}$; $U_C = U_B$. Ca1 occurs at (⅓, ⅔, ¼); for Ca2, z = ¼. For B, z = ¾. Mn occurs at (0, ½, 0); C occurs at (0, 0, *z*), for O1, z = ¼; for O2, z = ¾.

TABLE 3. GAUDEFROYITE: SELECTED INTERATOMIC DISTANCES (Å) AND ANGLES (°)

Bonds/T (°C)	25*	25	59	93	145	196	247	298	350	384	401	452	486
Ca1-O1 ×3	2.338(3)	2.346(4)	2.343(4)	2.346(4)	2.343(4)	2.344(4)	2.344(4)	2.343(4)	2.345(4)	2.344(4)	2.347(4)	2.349(4)	2.356(4)
Ca1-O3 ×6	2.587(2)	2.556(3)	2.560(3)	2.563(3)	2.566(3)	2.570(3)	2.575(3)	2.580(3)	2.586(3)	2.588(3)	2.590(3)	2.597(3)	2.601(3)
<Ca1-O>	**2.504(1)**	**2.486(1)**	**2.488(1)**	**2.491(1)**	**2.491(1)**	**2.495(1)**	**2.498(1)**	**2.501(1)**	**2.505(1)**	**2.506(1)**	**2.509(1)**	**2.515(1)**	**2.519(1)**
Ca2-O1 ×1	2.329(3)	2.348(4)	2.349(4)	2.350(4)	2.352(4)	2.354(4)	2.354(4)	2.358(4)	2.359(4)	2.361(4)	2.362(4)	2.363(4)	2.359(5)
Ca2-O2 ×1	2.385(3)	2.362(5)	2.366(5)	2.366(5)	2.369(5)	2.373(5)	2.377(5)	2.378(5)	2.379(5)	2.382(5)	2.383(5)	2.389(5)	2.400(6)
Ca2-O3 ×2	2.373(2)	2.409(4)	2.411(3)	2.413(3)	2.413(3)	2.418(4)	2.418(4)	2.420(4)	2.422(4)	2.423(4)	2.423(4)	2.423(4)	2.417(4)
Ca2-O_{Ca} ×2	2.368(5)	2.373(6)	2.375(6)	2.372(5)	2.372(6)	2.364(6)	2.368(6)	2.367(6)	2.366(6)	2.354(6)	2.353(6)	2.343(6)	2.315(6)
Ca2-O_{Cb} ×2	2.489(5)	2.575(11)	2.579(11)	2.579(11)	2.586(11)	2.587(12)	2.595(12)	2.600(12)	2.605(12)	2.610(13)	2.612(13)	2.619(13)	2.653(15)
Ca2-O_{Cc} ×2	2.736(6)	2.659(11)	2.657(11)	2.663(11)	2.665(11)	2.671(11)	2.676(12)	2.684(12)	2.699(12)	2.709(13)	2.715(13)	2.725(13)	2.721(16)
<Ca2-O>	**2.465(1)**	**2.474(2)**	**2.476(2)**	**2.477(2)**	**2.479(2)**	**2.481(3)**	**2.484(3)**	**2.488(3)**	**2.492(3)**	**2.494(3)**	**2.495(3)**	**2.497(3)**	**2.497(3)**
B-O2 ×1	1.460(7)	1.384(12)	1.393(11)	1.385(12)	1.393(11)	1.375(12)	1.383(12)	1.375(12)	1.373(12)	1.368(13)	1.370(12)	1.361(13)	1.333(15)
B-O3 ×2	1.393(4)	1.448(7)	1.442(6)	1.447(7)	1.444(6)	1.453(7)	1.444(6)	1.449(7)	1.452(7)	1.455(7)	1.454(7)	1.455(7)	1.468(8)
<B-O>	**1.415(2)**	**1.427(3)**	**1.426(3)**	**1.426(3)**	**1.427(3)**	**1.427(3)**	**1.424(3)**	**1.424(3)**	**1.426(3)**	**1.426(3)**	**1.426(3)**	**1.424(3)**	**1.423(4)**
C-O_C ×3	1.384(3)	1.326(4)	1.327(4)	1.328(4)	1.328(4)	1.335(4)	1.326(4)	1.328(5)	1.327(5)	1.333(5)	1.327(5)	1.329(5)	1.340(5)
Mn-O1 ×2	1.871(2)	1.862(2)	1.864(2)	1.864(2)	1.866(2)	1.867(2)	1.867(2)	1.867(2)	1.868(2)	1.868(3)	1.867(2)	1.867(2)	1.868(3)
Mn-O2 ×2	2.208(3)	2.216(3)	2.216(3)	2.219(3)	2.220(3)	2.222(3)	2.230(3)	2.233(3)	2.237(3)	2.238(3)	2.239(3)	2.242(3)	2.237(4)
Mn-O3 ×2	1.958(2)	1.929(3)	1.932(3)	1.932(3)	1.934(3)	1.934(3)	1.939(3)	1.940(3)	1.941(3)	1.943(3)	1.942(3)	1.946(3)	1.952(3)
<Mn-O>	**2.012(1)**	**2.003(1)**	**2.004(1)**	**2.005(1)**	**2.006(1)**	**2.008(1)**	**2.012(1)**	**2.013(1)**	**2.015(1)**	**2.016(1)**	**2.016(1)**	**2.018(1)**	**2.019(1)**
O_C-C-O_C ×3	119.99(3)	119.9(1)	119.8(1)	119.9(1)	119.8(1)	119.7(1)	119.9(1)	119.8(1)	119.7(2)	119.8(1)	119.8(1)	119.8(1)	120.0(1)
O2-B-O3 ×2	117.2(3)	121.0(5)	120.7(5)	121.1(5)	120.8(5)	121.6(5)	121.1(5)	121.5(5)	121.7(5)	121.9(5)	121.9(5)	122.1(5)	122.7(6)
O3-B-O3 ×1	125.2(5)	117.6(10)	118.2(10)	117.4(10)	118.0(10)	116.5(10)	117.5(10)	116.7(10)	116.2(10)	115.8(10)	115.9(10)	115.5(10)	114.1(12)
<O-B1-O>	**119.9(3)**	**119.9(6)**	**119.9(6)**	**119.9(6)**	**119.9(6)**	**119.9(6)**	**119.9(6)**	**119.9(6)**	**119.9(6)**	**119.9(6)**	**119.9(6)**	**119.9(6)**	**119.8(7)**
O1-Mn-O1 ×1	179.97(0)	179.98(0)	179.98(0)	179.96(0)	179.96(0)	180.00(0)	179.97(0)	179.97(0)	180.00(0)	179.97(0)	180.00(0)	180.00(0)	180.00(0)
O3-Mn-O3 ×1	180.00(0)	180.00(0)	179.97(0)	179.97(0)	179.98(0)	180.00(0)	179.96(0)	179.96(0)	180.00(0)	179.95(0)	180.00(0)	179.95(0)	179.98(0)
O1-Mn-O3 ×2	90.58(9)	91.20(12)	91.24(11)	91.16(11)	91.29(11)	91.24(11)	91.21(11)	91.25(11)	91.22(12)	91.27(12)	91.17(12)	91.03(12)	90.75(13)
O1-Mn-O3 ×2	89.42(9)	88.80(12)	88.76(11)	88.84(11)	88.71(11)	88.76(11)	88.79(11)	88.75(11)	88.78(12)	88.73(12)	88.83(12)	88.97(12)	89.25(13)
<O-Mn-O>	**90.00(3)**	**90.00(4)**	**90.00(4)**	**90.00(4)**	**90.00(4)**	**90.00(4)**	**90.00(4)**	**90.00(4)**	**90.00(4)**	**90.00(4)**	**90.00(4)**	**90.00(4)**	**90.00(4)**

* Data from HRPXRD.

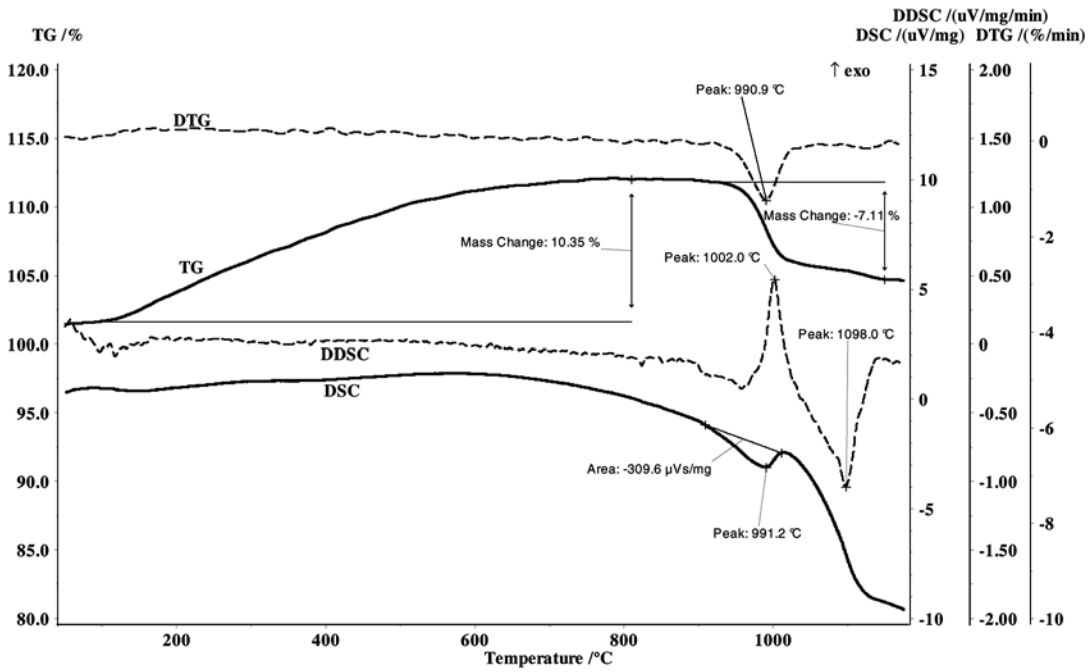

FIG. 5. Thermal analyses: TG, DTG, DSC, and DDSC curves for gaudefroyite, together with characteristic data.

Fig. 8a). However, all the Mn–O bonds are nearly constant with T (Fig. 8a).

The average <Ca1–O> and <Ca2–O> distances increase linearly with T (Table 3, Fig. 8b). The average <Ca1–O> distance increases slightly more than the average <Ca2–O> distance. The Ca2–O (= O1, O3) distances are short and nearly constant with T, whereas the short Ca2–O2 distance increases only slightly (Fig. 8b). However, the Ca2–O_C distances [two long distances (b, c) increase and one short distance (a) decreases] vary significantly with T (Fig. 8b). Because the O_C atoms belong to the CO_3^{2-} groups that occur in the channels of the structure, the Ca2–O_C distances, and the Ca2 site that also occurs in the channels (Fig. 1), will have an insignificant effect on the expansion of the structure. For the Ca1 site, the short Ca1–O1 distance is nearly constant with T, whereas the longer Ca1–O3 distance increases significantly and linearly with T, and is mainly responsible for the expansion of the structure (Fig. 8b). It appears that the exsolution in gaudefroyite occurs because of the high strain in the long Ca1–O3 distances at high T, and when exsolution occurs, the strain probably is released. There are six equal Ca1–O3 distances, and these bonds are directed in three-dimensional space and not located in any particular plane, so the expansion of the hexagonal structure is nearly isotropic.

The results in this study indicate that above 486°C, a minor amount of an exsolved phase occurs within the gaudefroyite host. This minor exsolved phase remains to be identified, but hausmannite appears to be a good candidate. Because it gives rise to few additional reflections (other reflections may overlap with those from gaudefroyite), we could not identify it convincingly by XRD. Additional data from chemical analysis and SEM may be necessary to identify the exsolved phase.

ACKNOWLEDGEMENTS

We thank the reviewers, R.F. Martin, O.V. Yakubovich, and an anonymous reviewer for useful comments. This research was carried out in part at the National Synchrotron Light Source, Brookhaven National Laboratory (BNL), beamline X7B, which is supported by the U.S. Department of Energy, Division of Materials Sciences and Division of Chemical Sciences, under Contract No. DE–AC02–98CH10886. HRPXRD data were collected at beamline 11–BM, Advanced Photon Source, Argonne National Laboratory. Use of the Advanced Photon Source was supported by the U. S. Department of Energy, Office of Science, Office of Basic Energy Sciences, under Contract No. DE–AC02–06CH11357.

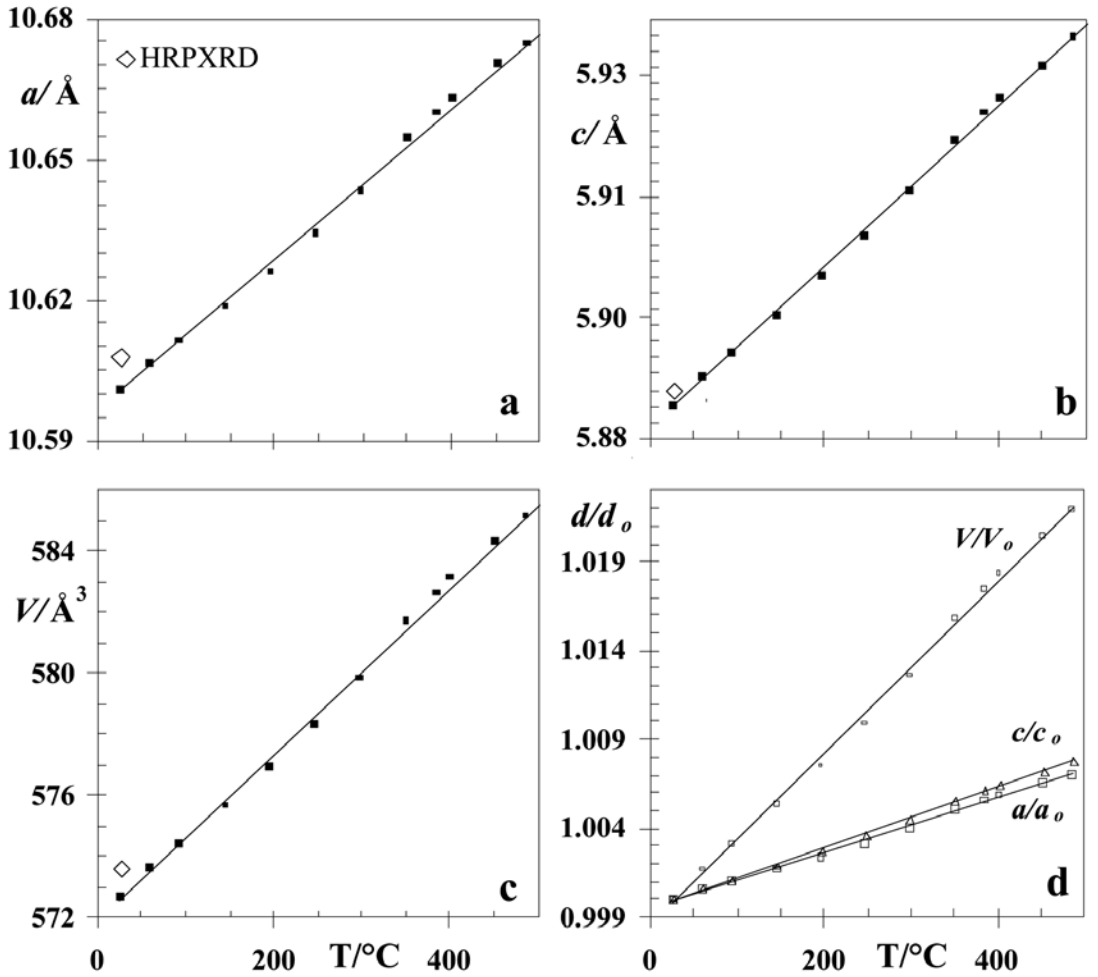

FIG. 6. The variation of the unit-cell parameters for gaudefroyite with temperature: (a) a, (b) c, (c) V, and (d) the ratio d/d_0. All parameters increase linearly on heating. Error bars are smaller than the symbols. Open diamonds are from HRPXRD data.

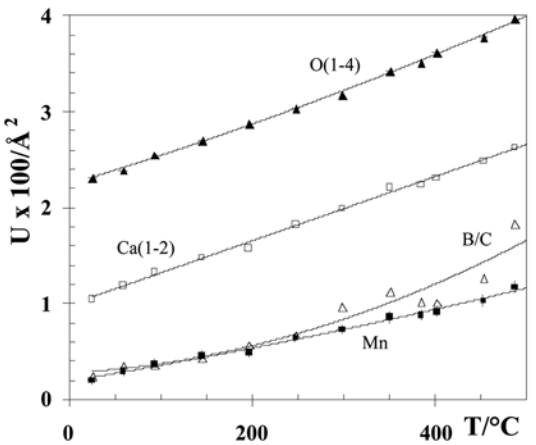

FIG. 7. Isotropic displacement parameters for gaudefroyite: all parameters increase with temperature.

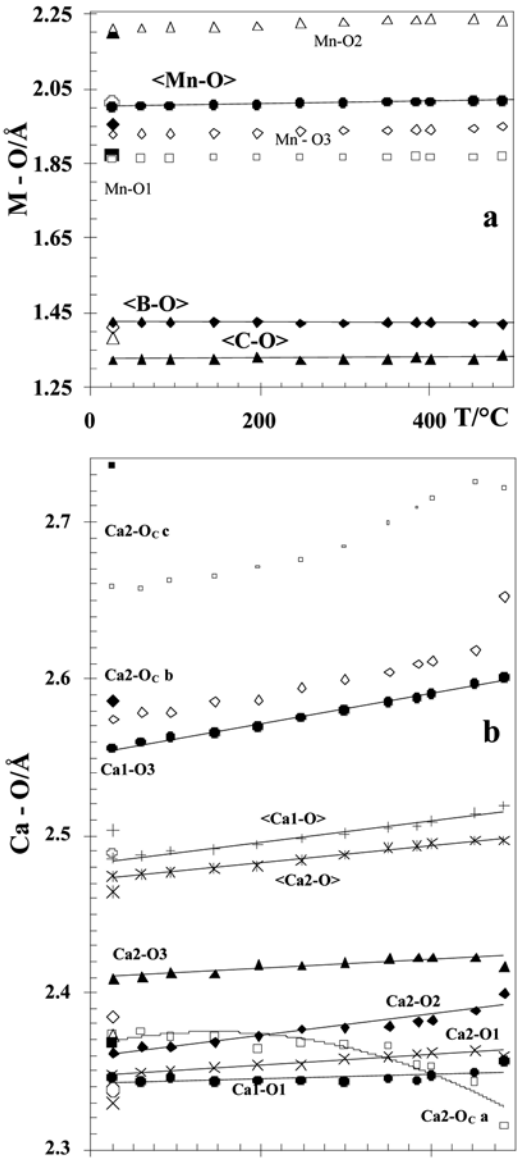

FIG. 8. Variation of bond distances with temperature in gaudefroyite. The HRPXRD data at 25°C are displayed using opposite symbols, *e.g.,* if the high-T data are shown as a solid symbol, the HRPXRD data are shown as an open symbol, or in a larger size.

REFERENCES

BEUKES, G.J., DE BRUIYN, H. & VAN DER WESTHUIZEN, W.A. (1993): Gaudefroyite from the Kalahari manganese field, South Africa. *Neues Jahrb. Mineral., Monatsh.*, 385-392.

GRANGER, M.M. & PROTAS, J. (1965): Détermination de la structure de la gaudefroyite. *C.R. Acad. Sci.* **260**, 4553-4555.

GRUNDY, H.D. & HASSAN, I. (1982): The crystal structure of a carbonate-rich cancrinite. *Can. Mineral.* **20**, 239-251.

HAMMERSLEY, A.P., SVENSSON, S.O., HANFLAND, M., FITCH, A.N. & HAUSERMANN, D. (1996): Two-dimensional detector software: from real detector to idealised image to two-theta scan. *High Pressure Research* **14**, 235-248.

HASSAN, I. (1996): The thermal behavior of cancrinite. *Can. Mineral.* **34**, 893-900.

HASSAN, I. (2000): Transmission electron microscopy study of gaudefroyite, $Ca_8Mn_6^{3+}[(BO_3)_6(CO_3)_2O_6]$. *Am. Mineral.* **85**, 1188-1194.

HASSAN, I. & BUSECK, P.R. (1992): The origin of the superstructure and modulations in cancrinite. *Can. Mineral.* **30**, 49-59.

HASSAN, I. & DUANE, M.J. (1999): The differential thermal analysis of gaudefroyite. *Can. Mineral.* **37**, 1363-1368.

HOCHLEITNER, R. (1986): Neufund von Gaudefroyit-kristallen in Südafrika. *Lapis* **11**(6), 19-20.

HODGMAN, C.D. (1955): *Handbook of Chemistry and Physics.* Chemical Rubber Publishing Co., Cleveland, Ohio.

HOFFMANN, C., ARMBRUSTER, T. & KUNZ, M. (1997): Structure refinement of (001) disordered gaudefroyite $Ca_8Mn_6^{3+}[(BO_3)_6(CO_3)_2O_3]$: Jahn–Teller-distortion in edge-sharing chains of $Mn^{3+}O_6$ octahedra. *Eur. J. Mineral.* **9**, 7-19.

JOURAVSKY, G. & PERMINGEAT, F. (1964): La gaudefroyite, une nouvelle espèce minérale. *Bull. Soc. Fr. Minéral. Cristallogr.* **87**, 216-229.

LARSON, A.C. & VON DREELE, R.B. (2000): *General Structure Analysis System* (GSAS). Los Alamos National Laboratory, Rep. **LAUR 86-748.**

TOBY, B.H. (2001): EXPGUI, a graphical user interface for GSAS. *J. Appl. Crystallogr.* **34**, 210-221.

YAKUBOVICH, O.V., SIMONOV, M.A. & BELOV, N.V. (1975): Refinement of crystal-structure of gaudefroyite, $Ca_4Mn_3^{3+}O_3(BO_3)_3(CO_3)$. *Kristallografiya* **20**, 152-155.

Received March 19, 2007, revised manuscript accepted January 15, 2008.